

The 2021 outburst of RS Oph. A pictorial atlas of the spectroscopic evolution: the first 18 days

Ulisse Munari¹ and Paolo Valisa²

1: INAF National Institute of Astrophysics, 36012 Asiago, Italy

2: ANS Collaboration, c/o Astronomical Observatory, 36012 Asiago, Italy

Abstract. *A pictorial atlas of the spectroscopic evolution at optical wavelengths is presented for the first 18 days of the 2021 outburst of the recurrent nova RS Oph, prior to the emergence of high ionization emission lines. The spectra presented here have been obtained at daily cadence with the Asiago 1.22m + B&C (3200-7900 Å, 2.3 Å/pix) and Varese 0.84m + Echelle telescopes (4250-8900 Å, resolving power 18,000). The spectra have been fully calibrated in IRAF, absolutely fluxed, and heliocentric corrected. The Echelle spectra have been also corrected for telluric absorptions.*

INTRODUCTION

The recurrent nova and symbiotic binary RS Oph underwent a new outburst in August 2021, following previous ones recorded in 1898, 1933, 1958, 1967, 1985 and 2006. At each new event a better coverage of the eruption was obtained with observations progressively expanding to cover the whole electromagnetic spectrum. For the 2006 event, an impressive amount of data has been gathered, and the book *RS Ophiuchi (2006) and the Recurrent Nova Phenomenon* edited by Bode, O'Brien & Darnley (2008, ASPC 401) provides a detailed summary of the main results.

Yet, a comprehensive and detailed mapping of the spectral evolution at optical wavelengths seems missing, at least at the level of completeness, detail and homogeneity of the present atlas. It aims to fill the gap, by providing a quick pictorial guide to the spectral evolution of RS Oph during the first 18 days of the 2021 outburst. To make the atlas promptly available, we just describe how the observations have been collected and how the reduced spectra have been incorporated in the atlas. This is of course no substitute for a proper analysis, to be carried out in due time. The latter will benefit from continued observations covering the rest of the evolution of RS Oph as well as comparison with the results of observations carried out at other wavelengths (and not yet published).

While presenting this first batch of spectra, our monitoring of RS Oph will continue at daily cadence for as long as possible, and updates to this atlas are planned for later epochs.

The current atlas covers the first 18 days of the eruption (August 8 to 26), those characterized by low ionization conditions. From day +19 (August 27), the evolution has progressed to the emergence of higher ionization lines (HeII, [FeVII]) as reported by Shore et al. (2021b,c).

The current outburst has triggered observations of RS Oph over the whole electromagnetic spectrum. Preliminary reports have been presented by Cheung et al. (2021a,b) and Wagner & HESS Collaboration (2021a,b) for γ -rays; Enoto et al. (2021a,b), Ferrigno et al. (2021), Luna et al. (2021), Page (2021), Page et al. (2021), Rout et al. (2021) and Shidatsu et al. (2021) for the X-rays; Mikolajewska et al. (2021), Munari U., Valisa P., (2021a,b), Shore et al. (2021a,b,c), and Taguchi et al. (2021a,b) for the optical; Woodward et al. (2021) for the infrared; and Sokolovsky et al. (2021) and Williams et al. (2021) for the radio. The results of the search for neutrino emission has been given by Pizzuto et al. (2021), and on the polarization of optical light by Nikolov & Luna (2021). A great summary of the main results obtained on the previous outburst of RS Oph in 2006 is the conference proceedings edited by Evans et al. (2008).

OBSERVATIONS

RS Oph has been observed each day for the first 18 days of its 2021 eruption with the Echelle slit-spectrograph mounted on the Varese 0.84m telescope. The spectra have been recorded over the range 4250-8900 Å, at a 18,000 resolving power. The data reduction has been performed in IRAF and has included all usual steps of correction for bias, dark and flat, sky subtraction, wavelength calibration (via Thorium lamp), and heliocentric correction. Spectrophotometric standards, located close on the sky to RS Oph, have been observed each night soon before and after the nova to achieve an optimal flux calibration, which was also essential to accurately merge the individual 30 Echelle orders into a single 1D fluxed spectrum not affected by dents at the points of jointure. Telluric dividers were observed each night

similarly to the spectrophotometric standards, to properly remove from the spectra of RS Oph the presence of telluric absorption lines. A journal of the Echelle observations is provided in Table 1. The poor quality of the spectrum for Aug 12 is due to cloud cover persisting all night.

RS Oph was also observed on almost each day for the first 18 days of its 2021 eruption with the B&C spectrograph attached to the Asiago 1.22m telescope, allowing to cover the 3200-7900 Å range at 2.3 Å/pix dispersion. The B&C spectra have been equally and fully reduced in IRAF and flux calibrated against spectrophotometric standards observed each night at a similar height on the horizon as RS Oph. A journal of the B&C observations is presented in Table 2.

At both telescopes a great emphasis has been put on maintaining the highest homogeneity throughout the observing campaign on the instrument set-up, choice of standards, observation and data reduction procedures. Any difference between the spectra presented in this atlas is more intrinsic to RS Oph than due to any stage of the observing process.

THE ATLAS

Given the huge intensity of the emission lines displayed by RS Oph and the necessity to compact many different spectra on the same picture, we adopt to plot the spectra on all figure as the **logarithm of the flux** (in $\text{erg cm}^{-2} \text{s}^{-1} \text{Å}^{-1}$). Multi-epoch observations within the same night have been averaged into one single spectrum per night.

The sequence of B&C spectra is presented first, with Figure 1 covering the whole wavelength interval, and Figures 2 and 3 zooming on the blue and red portions respectively, with identification of the principal lines. A list of the emission lines identified in the spectrum for Aug 23 ($t - t_o = +15.28$ days) is given in Table 3.

Selected portions of the Echelle spectra then follow. In Figure 4 we present the evolution of $H\alpha$, and that of HeI 5876 follows in Figure 5. Figures 6 and 7 are devoted to cover $H\beta$ and the nearby FeII multiplet 42 and HeI lines at 4921 and 5015 Å. Finally, Figure 8, zooms on the sharp components displayed by $H\alpha$, $H\beta$, FeII #42 5018 and HeI 5015 on top of the much wider and stronger emission lines, and to the NaI 5890, 5896 Å doublet.

REFERENCE EPOCH

To identify the spectra through the various figures, we have labelled them according to the observing UT date as listed in Tables 1 and 2. In the same tables the time elapsed since the onset of the outburst ($t - t_o$) and since maximum brightness ($t - t_{\text{max}}$) in the V-band are listed.

The very quick rise to maximum has been covered by L.P. Lou and B. Wang with observations obtained with a Sony DSLR camera and reported to AAVSO (observer code WPIA). Extrapolating back their linear rise to intercept the $V=11.1$ mag quiescence brightness that RS Oph displayed on preceding days, set the time of eruption to:

$$t_o = 2459435.00 \text{ JD} \quad 2021 \text{ Aug } 08.50 \quad (\pm 0.01) \quad (1)$$

The time of passage at maximum V-band magnitude is less accurately determined. Again from the AAVSO light-curve, we estimate:

$$t_{\text{max}}^V = 2459436.18 \text{ JD} \quad 2021 \text{ Aug } 09.58 \quad (\pm 0.05) \quad (2)$$

ACKNOWLEDGMENTS

We express our gratitude to P. Ochner (Univ. Padova) and A. Vagnozzi (ANS Collaboration) for their help with the acquisition of some of the spectra used in this paper.

REFERENCES

- Cheung C. C., Ciprini S., Johnson T. J., 2021a, ATel, 14834
 Cheung C. C., Johnson T. J., Mereu I., et al., 2021b, ATel, 14845
 Enoto T., Maehara H., Orio M., et al., 2021a, ATel, 14850
 Enoto T., Orio M., Fabian A., et al., 2021b, ATel, 14864
 Evans A., Bode M. F., O'Brien T. J., Darnley M. J., eds., 2008, RS Ophiuchi (2006) and the Recurrent Nova Phenomenon, ASPC, 401
 Ferrigno C., Savchenko V., Bozzo E., et al., 2021, ATel, 14855
 Luna G. J. M., Jimenez-Carrera R., Enoto T., et al., 2021, ATel, 14872
 Mikolajewska J., Aydi E., Buckley D., et al., 2021, ATel, 14852

Munari U., Valisa P., 2021a, ATel, 14840
 Munari U., Valisa P., 2021b, ATel, 14860
 Nikolov Y., Luna G. J. M., 2021, ATel, 14863
 Page, K. L. 2021, ATel, 14885
 Page K. L., Osborne J. P., Aydi E., 2021, ATel, 14848
 Pizzuto A., Vandenbroucke J., Santander M., IceCube Collaboration, 2021, ATel, 14851
 Rout S. K., Srivastava M. K., Banerjee D. P. K., et al., 2021, ATel, 14882
 Shidatsu M., Negoro H., Mihara T., et al., 2021, ATel, 14846
 Shore S. N., Allen H., Bajer M., et al., 2021a, ATel, 14868
 Shore S. N., Teyssier F., Thizy O., 2021b, ATel, 14881
 Shore S. N., Teyssier F., Guarro J., et al., 2021c, ATel, 14883
 Sokolovsky K., Aydi E., Chomiuk L., et al., 2021, ATel, 14886
 Taguchi K., Ueta, T., Isogai, K., 2021a, ATel, 14838
 Taguchi K., Maheara H., Isogai K., et al., 2021b, ATel, 14858
 Williams D., O'Brien T., Woudt P., et al., 2021, ATel, 14849
 Wagner, S. J., HESS Collaboration, 2021a, ATel, 14844
 Wagner, S. J., HESS Collaboration, 2021b, ATel, 14857
 Woodward C. E., Evans A., Banerjee D. P. K., et al., 2021, ATel, 14866

Table 1: Journal of Echelle spectroscopic observations obtained with the Varese 0.84m telescope.

date UT		expt (sec)	HJD (-2459400)	$t - t_0$ (days)	$t - t_{\max}$ (days)
yyyy-mm-dd	hh:mm				
2021-08-09	19:30	900	36.316	1.32	0.14
2021-08-09	20:03	540	36.339	1.34	0.16
2021-08-09	20:55	540	36.375	1.38	0.20
2021-08-09	21:41	360	36.407	1.41	0.23
2021-08-10	19:41	720	37.324	2.32	1.14
2021-08-10	21:21	720	37.393	2.39	1.21
2021-08-11	19:23	720	38.311	3.31	2.13
2021-08-11	20:11	1200	38.344	3.34	2.16
2021-08-12	19:50	1200	39.330	4.33	3.15
2021-08-13	19:31	900	40.316	5.32	4.14
2021-08-14	20:40	1440	41.364	6.36	5.18
2021-08-15	19:40	1200	42.323	7.32	6.14
2021-08-16	20:05	1500	43.338	8.34	7.16
2021-08-17	19:20	900	44.309	9.31	8.13
2021-08-18	19:30	1500	45.315	10.32	9.14
2021-08-19	20:31	1500	46.358	11.36	10.18
2021-08-20	19:28	1500	47.314	12.31	11.13
2021-08-21	19:18	1500	48.307	13.31	12.13
2021-08-22	19:20	1500	49.308	14.31	13.13
2021-08-23	19:45	2400	50.325	15.33	14.15
2021-08-24	19:41	1800	51.323	16.32	15.14
2021-08-25	19:15	1800	52.304	17.30	16.12
2021-08-26	19:10	2400	53.301	18.30	17.12

Table 2: Journal of B&C spectroscopic observations obtained with the Asiago 1.22m telescope.

date UT		expt (sec)	HJD (-2459400)	$t - t_0$ (days)	$t - t_{\max}$ (days)
yyyy-mm-dd	hh:mm				
2021-08-09	18:49	100	36.284	1.28	0.10
2021-08-09	19:56	150	36.331	1.33	0.15
2021-08-10	19:11	120	37.300	2.30	1.12
2021-08-10	21:11	150	37.383	2.38	1.20
2021-08-11	19:09	90	38.298	3.30	2.12
2021-08-11	22:03	130	38.419	3.42	2.24
2021-08-12	18:44	90	39.281	4.28	3.10
2021-08-12	19:05	170	39.295	4.30	3.12
2021-08-12	20:45	120	39.365	4.37	3.19
2021-08-13	19:39	120	40.319	5.32	4.14
2021-08-13	21:04	120	40.378	5.38	4.20
2021-08-14	20:24	100	41.351	6.35	5.17
2021-08-15	20:11	120	42.342	7.34	6.16
2021-08-15	21:16	90	42.386	7.39	6.21
2021-08-17	19:13	120	44.301	9.30	8.12
2021-08-18	19:24	120	45.309	10.31	9.13
2021-08-19	18:44	110	46.281	11.28	10.10
2021-08-19	19:54	90	46.330	11.33	10.15
2021-08-20	19:22	120	47.307	12.31	11.13
2021-08-20	20:51	90	47.369	12.37	11.19
2021-08-22	19:42	150	49.321	14.32	13.14
2021-08-23	18:41	150	50.279	15.28	14.10

Table 3: Identification of emission lines in the Asiago 1.22m + B&C spectrum of RS Oph for Aug 23 ($t - t_0 = +15.28$ days).

λ	line	λ	line	λ	line	λ	line
3721	H14	4176	FeII 27+28	4823	HeI, FeII 42	5676	NII
3733	H13	4233	FeII 27	4949	[OIII]	5755	[NII]
3750	H12	4273	FeII 27	5007	[OIII]	5876	HeI
3770	H11	4300	FeII 27+28	5019	HeI+FeII 42	5991	FeII 46
3798	H10	4340	H γ	5048	HeI	6148	FeII 74
3837	H9	4363	[OIII]	5169	FeII 42	6248	FeII 74
3856	HeI	4388	HeI	5185	FeII	6318	FeII
3868	HeI	4417	FeII 27	5198	FeII 49	6369	blend
3889	H8+HeI	4471	HeI	5234	FeII 49	6433	FeII 40
3927	HeI	4489	FeII 37	5255	FeII 49	6456	FeII 74
3936	HeI	4520	FeII 37+38	5265	FeII 48	6563	H α
3970	H ϵ	4555	FeII 37+38	5276	FeII 49	6678	HeI
4026	HeI	4584	FeII 38	5316	FeII 48+49	7065	HeI
4070	FeII 22	4634	NIII+FeII 37	5363	FeII 48	7281	HeI
4101	H δ	4647	CIII	5426	FeII 49	7711	FeII 73
4124	FeII 22	4713	HeI	5496	FeII	7774	OI
4144	HeI	4861	H β	5535	FeII 55		

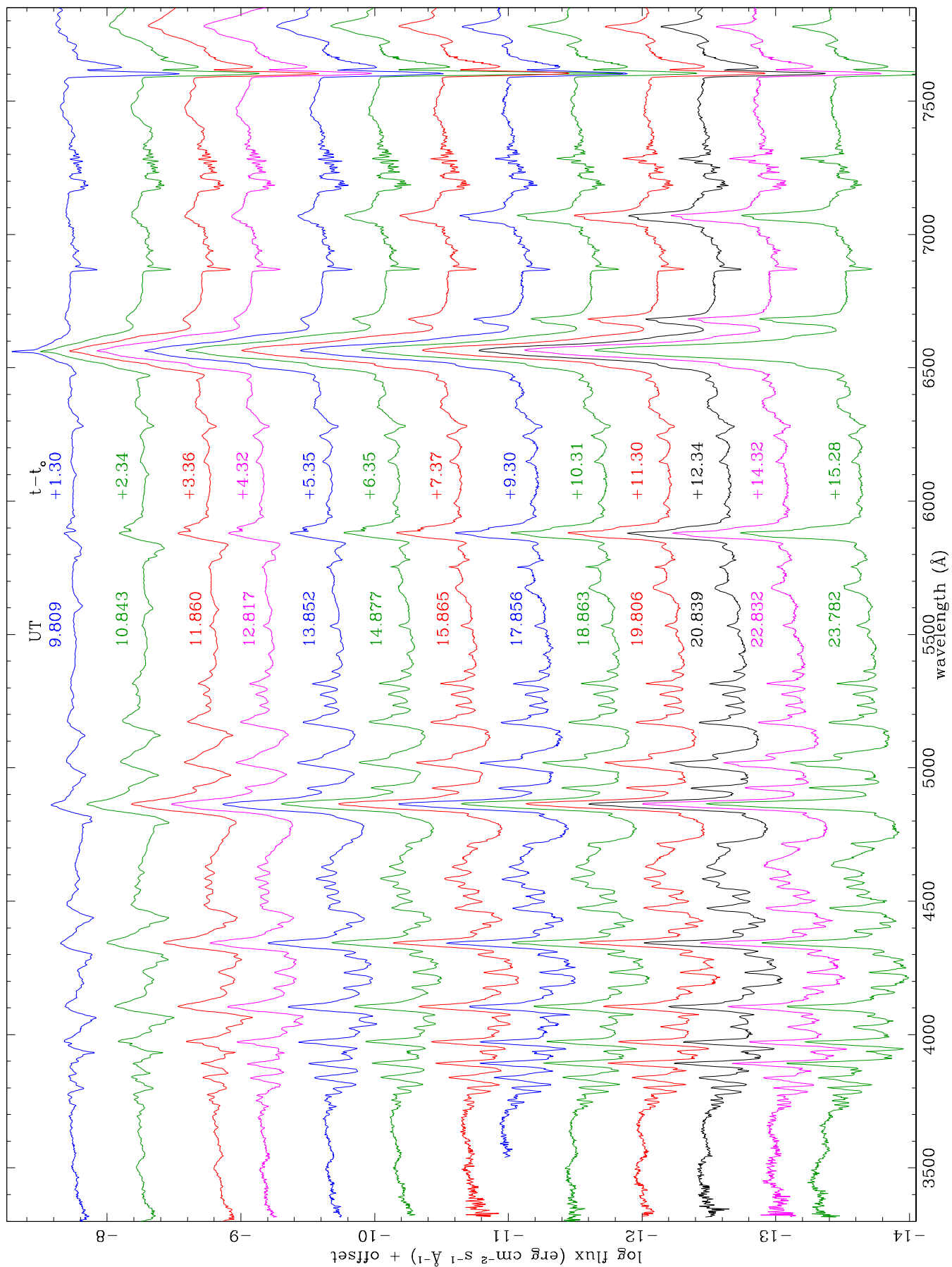


Figure 1: Sequence of Asiago 1.22m spectra showing the whole recorded range. The logarithm of the flux is adopted as the ordinates and a shift is applied to avoid overplotting.

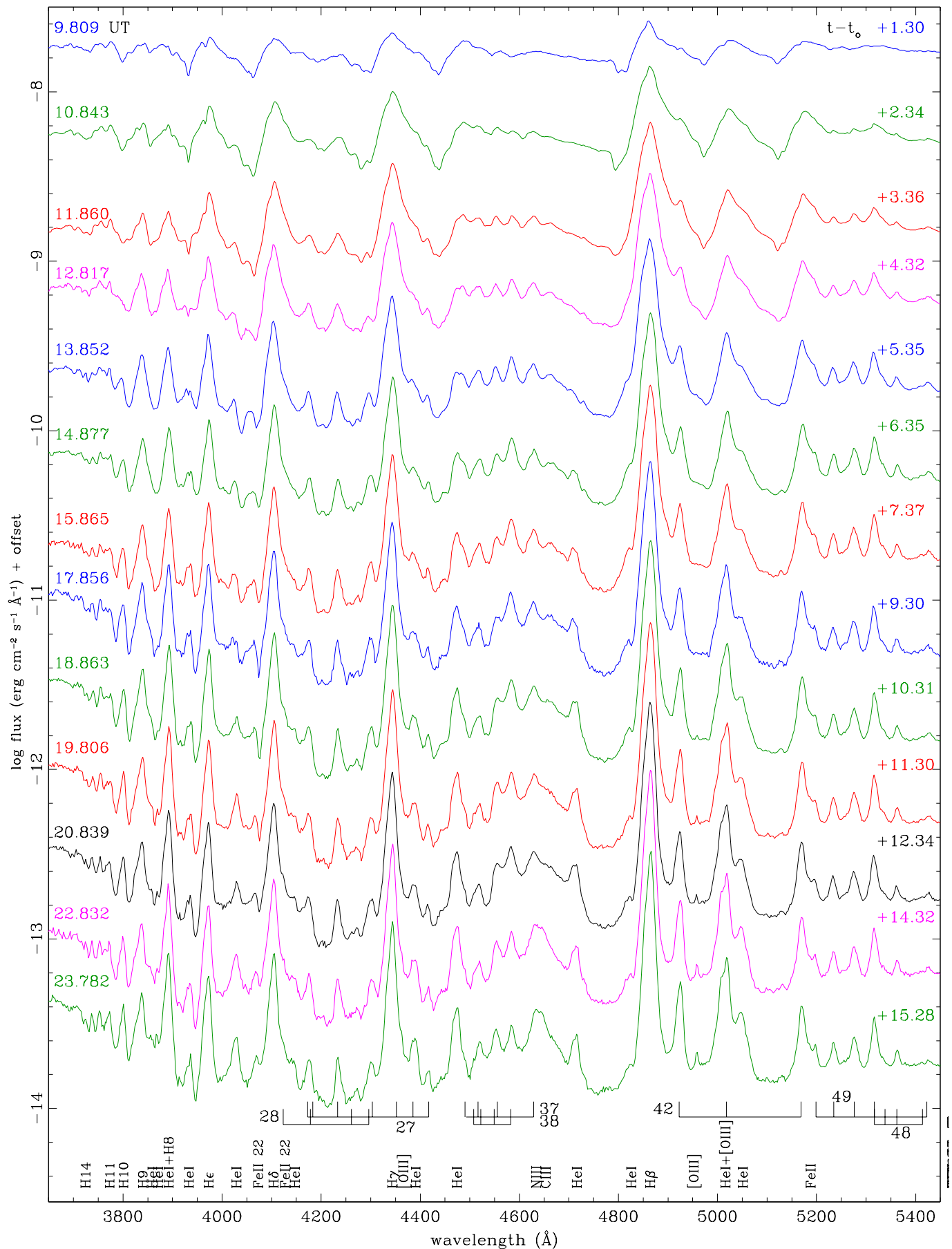


Figure 2: An expanded view of the 3650-5450 Å interval for the same spectra of Figure 1. The logarithm of the flux is adopted as the ordinates and a shift is applied to avoid overplotting.

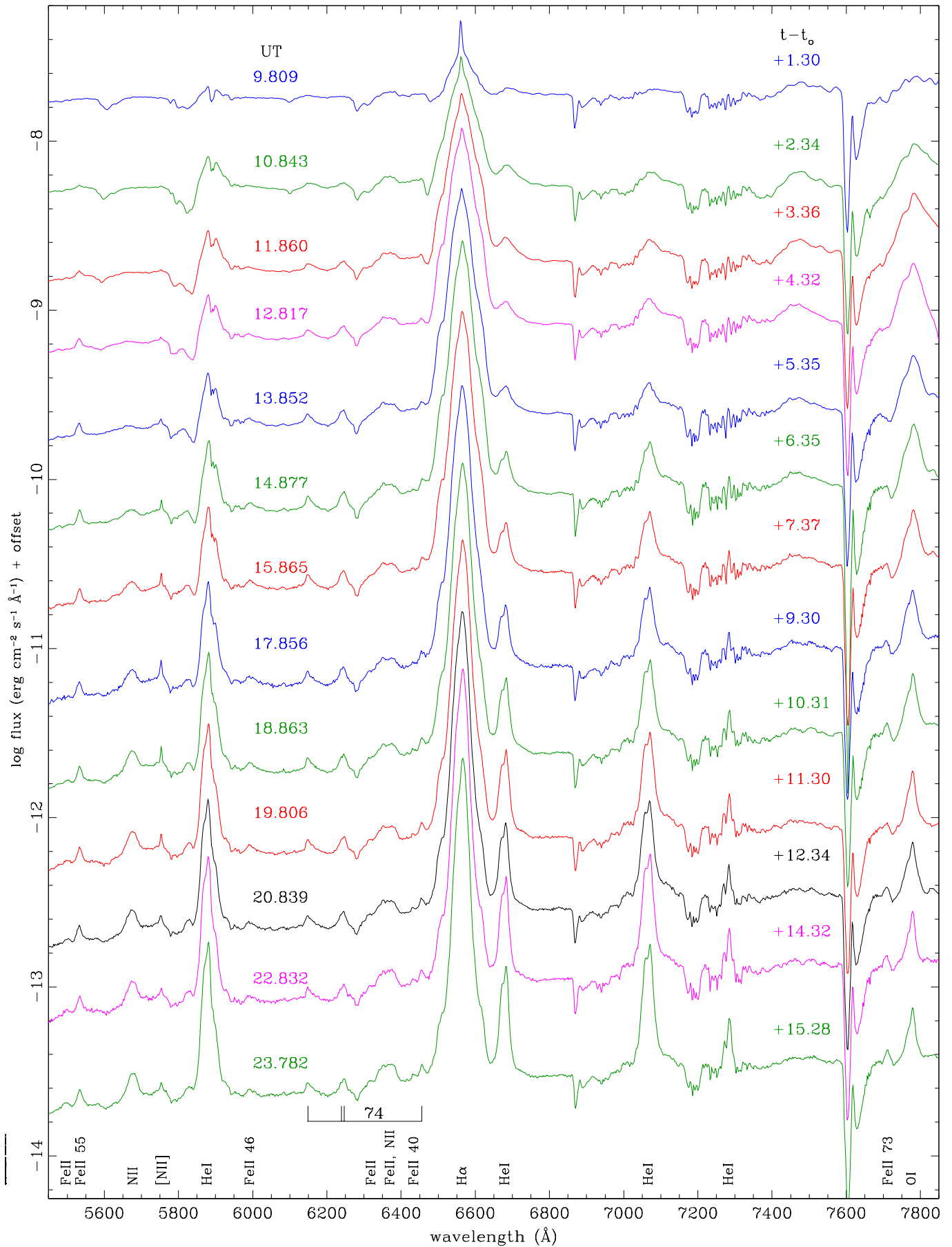


Figure 3: An expanded view of the 5450-7850 \AA interval for the same spectra of Figure 1. The logarithm of the flux is adopted as the ordinates and a shift is applied to avoid overplotting.

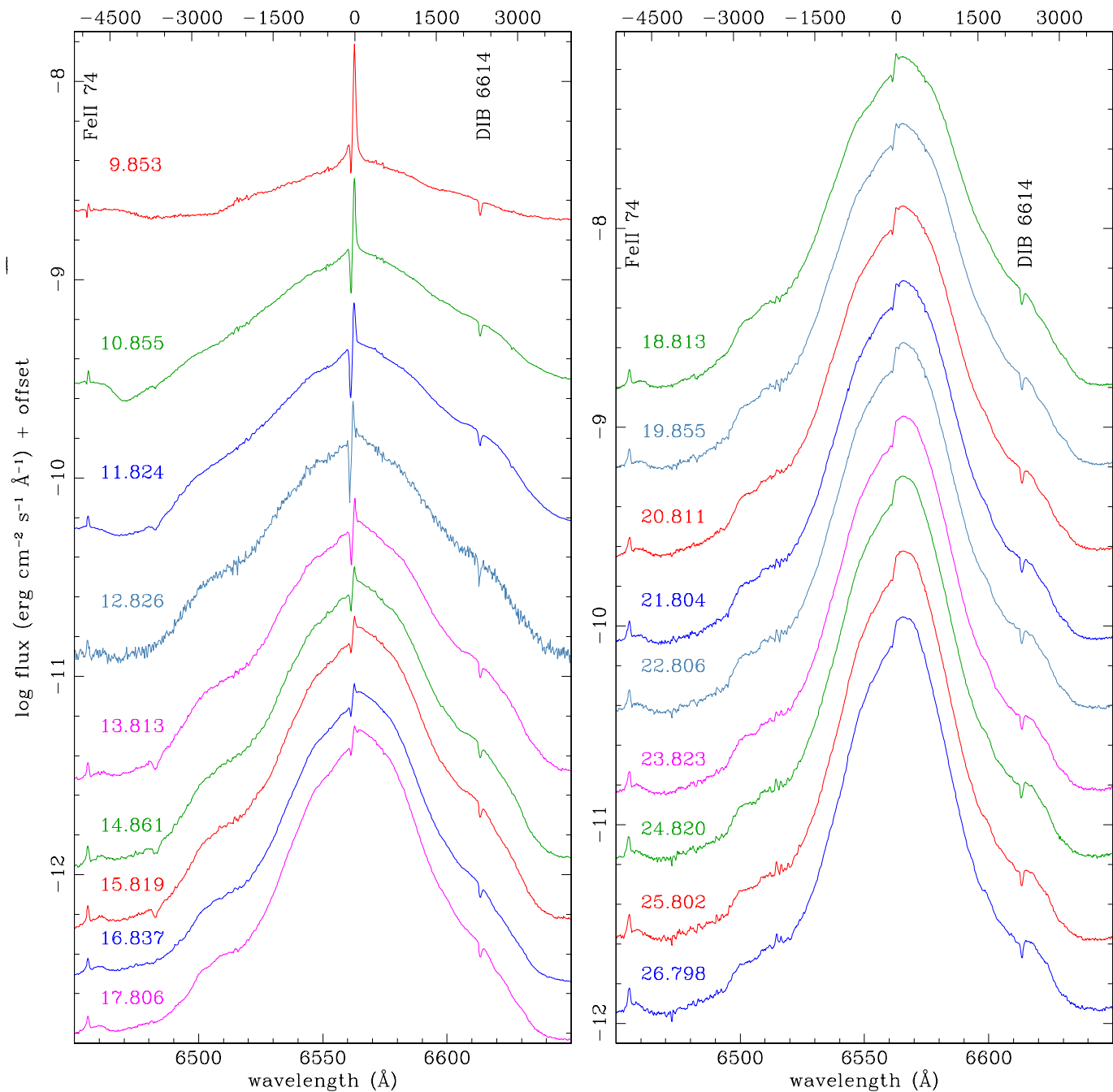


Figure 4: Evolution of the H α profile from Varese 0.84m Echelle spectra. The abscissae at the top give the heliocentric radial velocity (in km/s). The logarithm of the flux is adopted as the ordinates and a shift is applied to avoid overplotting.

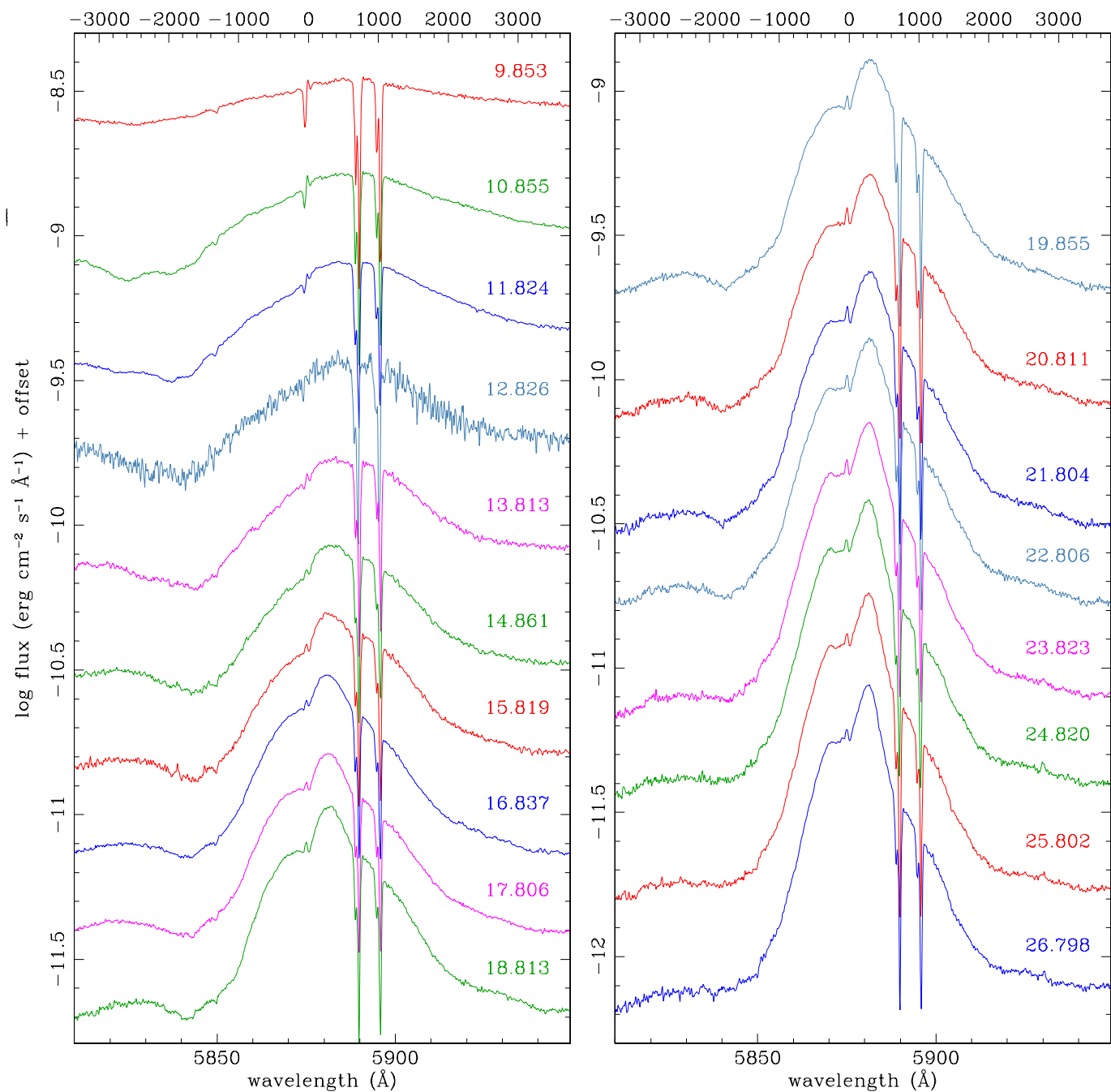


Figure 5: Evolution of the HeI 5876 profile and superimposed NaI doublet from Varese 0.84m Echelle spectra. The abscissae at the top give the heliocentric radial velocity (in km/s). The logarithm of the flux is adopted as the ordinates and a shift is applied to avoid overplotting.

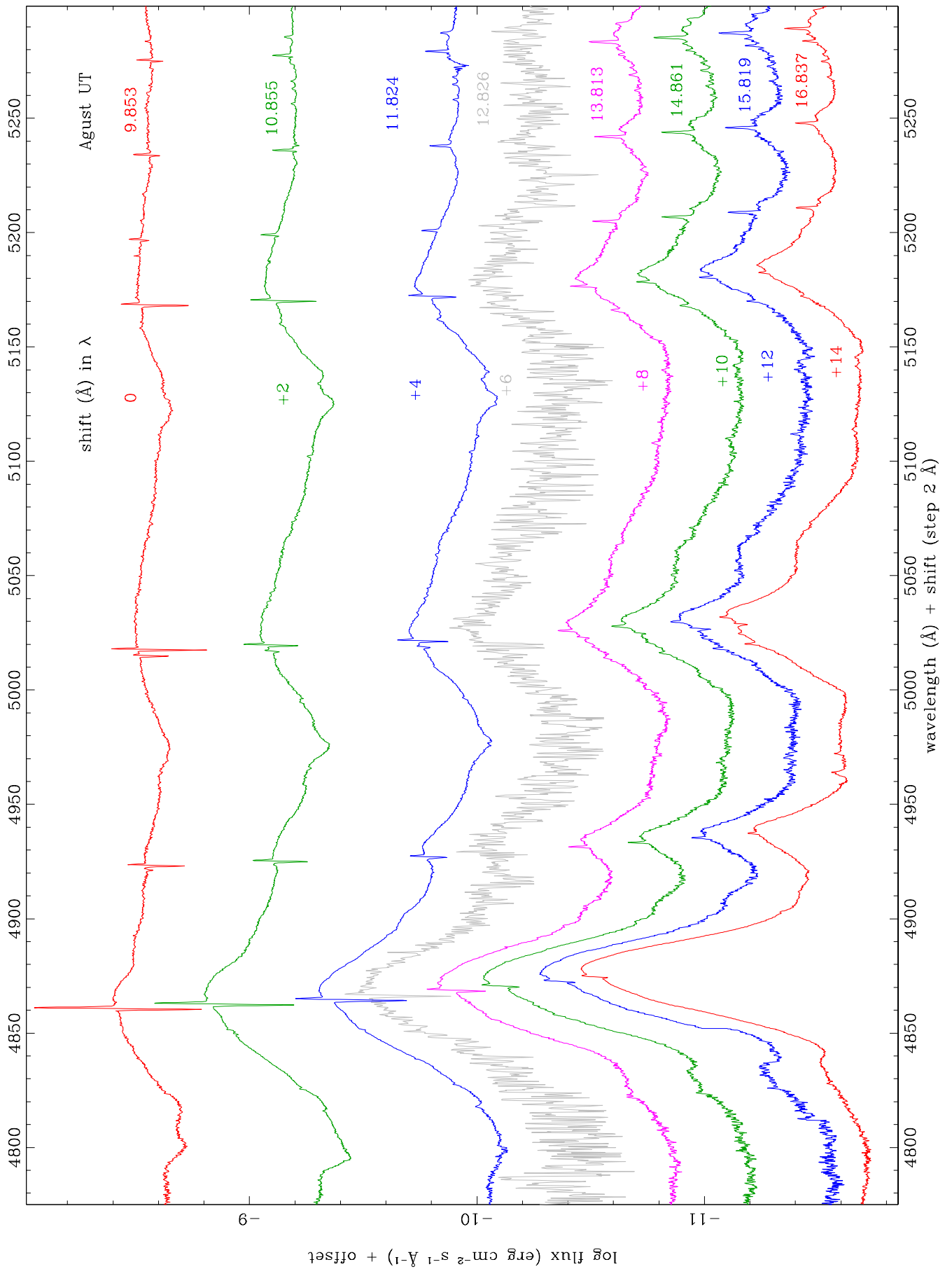


Figure 6: Series of Varese 0.84m Echelle spectra covering the $H\beta$, FeII multiplet 42 and HeI 4941, 5015 emission lines for the first eight days of the monitoring (the remaining dates are covered by the following Figure 7). The logarithm of the flux is adopted as the ordinates and a shift is applied to avoid overplotting.

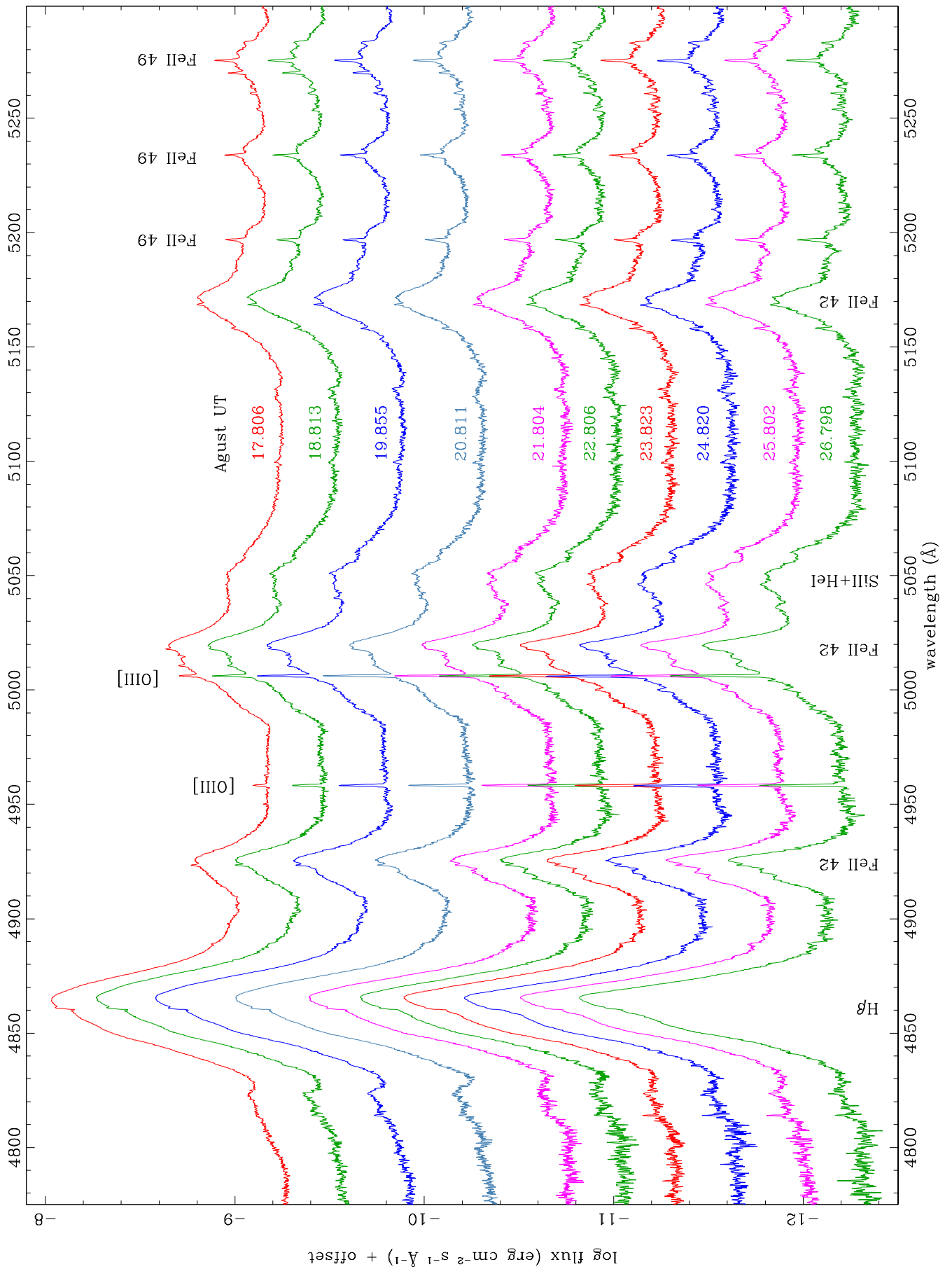


Figure 7: Series of Varese 0.84m Echelle spectra covering the $H\beta$, FeII multiplet 42 and HeI 4941, 5015 emission lines for the last ten days of our monitoring (the previous eight days are covered by preceding Figure 6). The logarithm of the flux is adopted as the ordinates and a shift is applied to avoid overplotting.

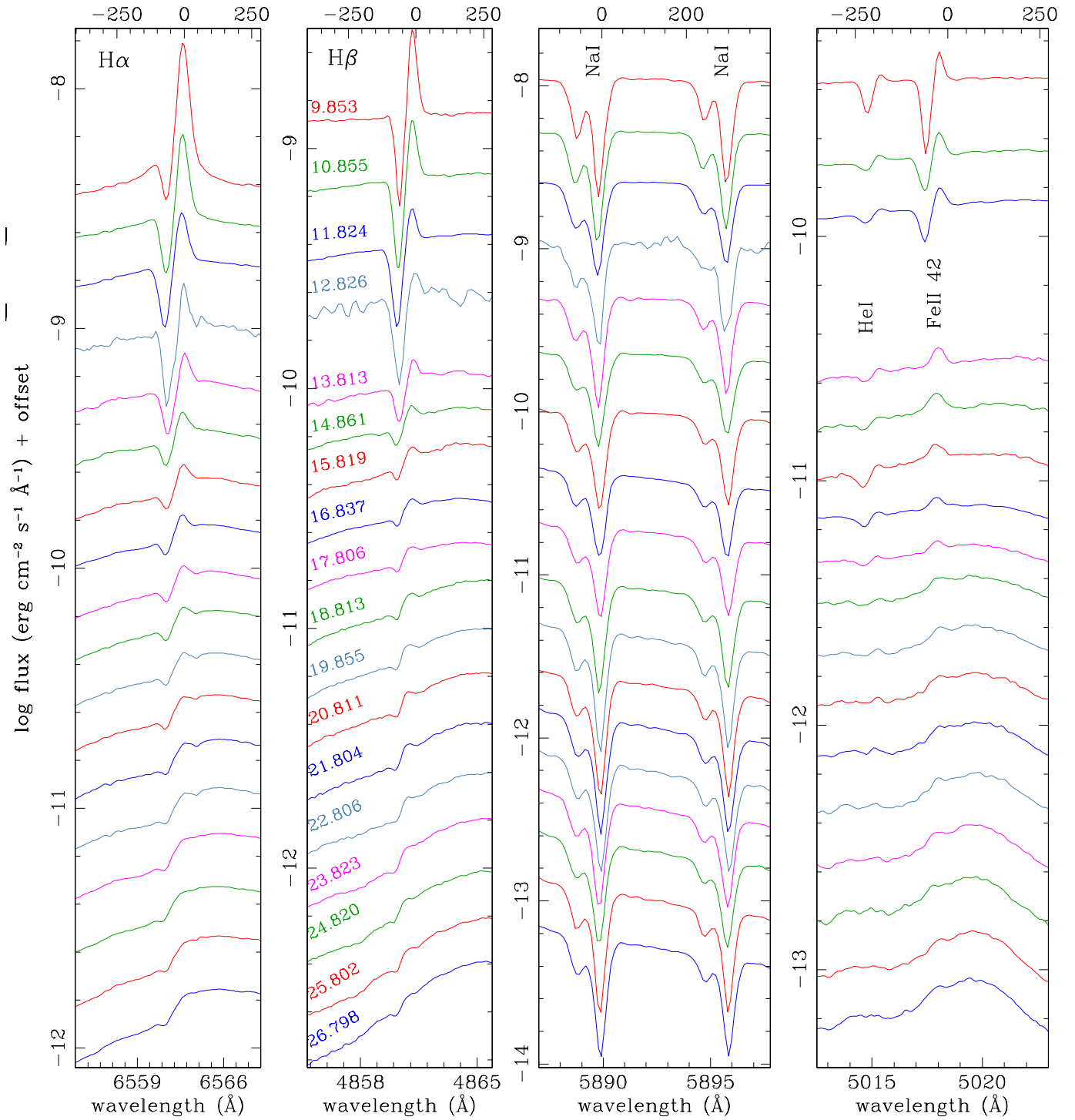


Figure 8: Evolution of the narrow components for H α , H β , HeI 5015 and FeII 5018, as well as the NaI doublet from Varese 0.84m Echelle spectra. The abscissae at the top give the heliocentric radial velocity (in km/s). The logarithm of the flux is adopted as the ordinates and a shift is applied to avoid overplotting.